### Title

Experimentally-based relaxation modulus of polyurea and its composites




### Journal

Mechanics of Time-Dependent Materials, 20(2)

### ISSN

1385-2000



### Authors

Jia, Zhanzhan
Amirkhizi, Alireza V
Nantasetphong, Wiroj
et al.



### Publication Date

2016-06-01

### DOI

10.1007/s11043-015-9289-1

Peer reviewed

**Published on Mechanics of Time-dependant Materials**

# Experimentally-based Relaxation Modulus of Polyurea and its Composites

**Zhanzhan Jia · Alireza V. Amirkhizi · Wiroj Nantasetphong · Sia Nemat-Nasser**

Received: 13 May 2015 / Accepted: 25 Dec 2015

**Abstract** Polyurea is a block copolymer that has been widely used in the coating industry as an abrasion-resistant and energy-dissipative material. Its mechanical properties can be tuned by choosing different variations of diamines and diisocyanates as well as by adding various nano and micro-inclusions to create polyurea-based composites. Our aim here is to provide the necessary experimentally-based viscoelastic constitutive relations for polyurea and its composites in a format convenient to support computational studies. The polyurea used in this research is synthesized by the reaction of Versalink P-1000 (Air Products) and Isonate 143L (Dow Chemicals). Samples of pure polyurea and polyurea composites are fabricated and then characterized using dynamic mechanical analysis (DMA). Based on the DMA data, master curves of storage and loss moduli are developed using time-temperature superposition. The quality of the master curves is carefully assessed by comparing with the ultrasonic wave measurements and by Kramers-Kronig relations. Based on the master curves, continuous relaxation spectra are calculated, then the time-domain relaxation moduli are approximated from the relaxation spectra. Prony series of desired number of terms for the frequency ranges of interest are extracted from the relaxation modulus. This method for developing cost efficient Prony series has been proven to be effective and efficient for numerous DMA test results of many polyurea/polyurea-based material systems, including pure polyurea with various stoichiometric ratios, polyurea with milled glass inclusions, polyurea with hybrid-nano particles and polyurea with phenolic microbubbles. The resulting viscoelastic models are customized for the frequency ranges of interest, reference temperature and desired number of Prony terms, achieving both computational accuracy and low cost. The method is not limited to polyurea-based systems. It can be applied to other similar polymers systems.

**Keywords** polyurea, master curves, Prony series, dynamic mechanical testing, time-temperature superposition, relaxation spectra

## 1 Introduction

Polyurea is the general name for a group of copolymers synthesized by the reaction of a diisocyanate component and a diamine component. It has shown remarkable thermal and mechanical properties and is commonly used as a coating material which is tough, abrasion-resistent and is capable of dissipating shock/ impact-induced energy.

In this study, polyurea is synthesized using Versalink P-1000 (Air Products and Chemicals, Inc.) and Isonate 143L (Dow Chemicals Co.), and the resultant material is a segmented copolymer which has hard domains dispersed in a soft matrix [Castagna et al., 2012, Rinaldi et al., 2011]. The $T_g$ of the soft domain is around $-60^{\circ}C$, which also is regarded as the $T_g$ of polyurea, and the $T_g$ of the hard domain is above $100\ ^{\circ}C$ [Rinaldi et al., 2011]. Due to the difference of the $T_g$ of the soft and hard segments, polyurea's behavior in the majority of its applications' conditions (temperature and frequencies of interest) may be likened to a lightly cross-linked elastomer reinforced by the nano-size hard domains[Castagna et al., 2012], which also serve as chemical and physical cross-link sites.

The wide transition zone of polyurea from rubbery state to glassy state makes the viscoelastic properties of polyurea highly sensitive to the temperature, pressure and strain rate [Qiao et al., 2011, Roland and Casalini, 2007, Sarva et al., 2007]. Throughout the transition zone of polyurea, its stiffness and loss modulus increase drastically from the rubbery state to the glassy state, which makes it an ideal protection material in the high strain rate loading conditions. These properties of polyurea makes its constitutive modeling rarther difficult. Comparing to the wide application of polyurea, the number of polyurea material models is limited [Grujicic et al., 2010]. The polyurea model in Ref. [Amirkhizi et al.,

Zhanzhan Jia (E-mail: z1jia@ucsd.edu) · Wiroj Nantasetphong · Sia Nemat-Nasser
Center of Excellence for Advanced Materials, Department of Mechanical and Aerospace Engineering
University of California, San Diego, La Jolla, CA, 92093-0416, USA

Alireza V. Amirkhizi
Department of Mechanical Engineering, University of Massachusetts, Lowell, MA, 01854, USA

2006] is a pressure/temperature-sensitive one based on the experimental data of time-domain measurement, where Prony series approximations of relaxation modulus are used to make large scale FEM calculations tractable.

Time-domain measurement is in general less accurate and more difficult to conduct than the dynamic mechanical analysis (DMA). In this study, a classical time-temperature superposition (TTS) is used to approximate the mechanical properties of polyurea using the dynamic mechanical analysis data, since directly measurement in such a broad frequency range is not readily available. Recognizing the conditions and the limitations of TTS, care is taken and quality assessments are applied to make sure the use of master curves is not arbitrary. Based on the DMA data, the classical TTS method is applied to develop the frequency-domain master curves which may span more than ten decades on the logarithmic scale.

In order to assess the quality of the master curve, it is compared with ultrasonic wave test data, and is also checked by Kramers-Kronig relations. The frequency-domain master curve is used to calculate the continuous relaxation spectrum, and then the time-domain relaxation modulus is obtained. Prony series of 4-8 terms are commonly used in the computational platforms. In Ref. [Amirkhizi et al., 2006], 4 Prony terms were used. But small number of Prony terms are not enough to accurately represent the material properties in the entire frequency range of 10 decades or more. Thus, customized Prony series of reduced number of terms are calculated for the specific computational problems to achieve both reliable accuracy and low computational cost.

The same data processing method has been successfully applied for various polyurea and polyurea-based composite systems developed in our lab. These include polyurea with different stoichiometric ratios, polyurea with milled glass inclusions, polyurea with hybrid nano particles and polyurea with phenolic microbubbles. For all these material systems, the stated method has shown great efficiency and consistency in generating the required Young's modulus viscoelastic properties, which is dominant by shear modulus ($E^* \simeq 3G^*$) for higher temperatures or long relaxation times near rubbery state.

This paper details this method using the data of pure polyurea and illustrates the final results in terms of two examples of the corresponding composites: polyurea with milled glass (PUMG) and polyurea with phenolic microbubbles (PUPMB). PUMG is an example of polyurea composites with rigid and high-density inclusions and PUPMB is an example with flexible and light-weight inclusions. The master curves of polyurea with various stoichiometric ratios can be found in [Holzworth et al., 2013], and the master curves of polyurea with hybrid nano particles will appear in a future publication.

The new contributions of this work are:

1) to develop an automated computational code to efficiently process experimental data of dynamic mechanical analysis to create the Prony series for the viscoelastic properties of polyurea and polyurea composites, suitable for computational platforms.

2) to use the Kramers-Kronig relations to assess the quality of the master curves.

3) to optimize creating the Prony series for the frequency range of interest that minimizes the computational cost.

We note that the presented method is applicable to various similar types of polymers and polymer composites, and is not limited to polyurea.

## 2 Sample fabrication

### 2.1 Pure polyurea sample fabrication

Polyurea is synthesized using Versalink P-1000 (Air Products and Chemicals, Inc.) and Isonate 143L (Dow Chemicals Co.). At room temperature, both components are liquid. The two components are degassed separately under vacuum at 1 torr and stirred by Teflon coated magnetic stir bars for 1 hour before being mixed together. The mixture is stirred for another 5 minutes under vacuum before transferring into the Teflon molds by disposable syringes. The stoichiometric ratio of the isocyanate to amine is standard 1.05 [Broekaert, 2002]. The samples are cured in an environmental chamber for 2 weeks before testing. In the chamber, the relative humidity is controlled at 10%.

### 2.2 Polyurea based composite materials sample fabrication

The two examples of polyurea composites are polyurea with milled glass (PUMG) and polyurea with phenolic microbubbles (PUPMB).

Milled glass is purchased from Fibertec, Inc. (product number 3032). Phenolic microbubbles are purchased from Fiberglass Supply. The particle density of the milled glass is $2.5 g/cm^3$, and the particle density of phenolic microbubbles is $0.23 g/cm^3$. The density of pure polyurea is $1.09 g/cm^3$.

Milled glass 3032 is made of E glass fiber. The average length of the particles is 200 $\mu m$, and the average diameter is 16 $\mu m$. The phenolic microbubbles are thin shell spheres made of phenol formaldehyde resin. The average shell thickness of the phenolic microbubbles is 1 $\mu m$, and the average diameter is 37 $\mu m$. The purpose of incorporating the milled glass into polyurea is increasing both the storage and loss moduli, while including the phenolic microbubbles can significantly reduce the material density.

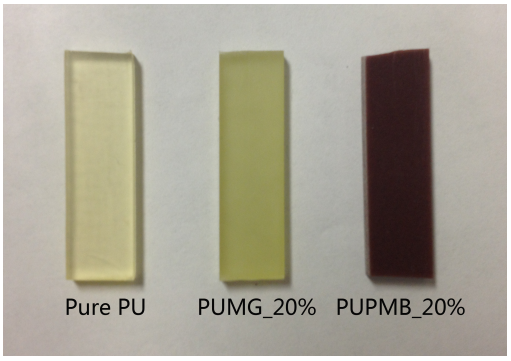


**Fig. 1** Cast samples of pure polyurea, polyurea with 20% volume fraction of milled glass (PUMG_20%), and polyurea with 20% volume fraction of phenolic microbubbles (PUPMB_20%).

During the fabrication, the filler material is first mixed with the more viscus component, which is the Versalink P-1000, before being degassed for 2 hours. After degassing, the appropriate amount of Isonate 143L (isocyanate to amine stoichiometric ratio 1.05) is added to the Versalink-filler mixture and stirred under vacuum for an extra 5 minutes before transferring into the Teflon molds using disposable syringes. Same as pure polyurea, the cast composites are cured in the environmental chamber for at least 2 weeks before testing. Fig.1 shows the dynamic mechanical analysis samples of pure polyurea, polyurea with 20% volume fraction of milled glass and polyurea with 20% volume fraction of phenolic microbubbles.

## 3 Dynamic mechanical analysis (DMA)

Dynamic mechanical analysis is performed using the TA Instrument Dynamic Mechanical Analyzer 2980. Single-cantilever bending tests are conducted, and DMA data are collected using the corresponding TA data analysis software.

In the single cantilever bending test, the complex dynamic Young's modulus $E^*$ is acquired. It can be written as $E^* = E' + iE''$. $E'$ is the storage modulus, representing the stiffness of the material, and $E''$ is the loss modulus, representing the capability for the material to dissipate mechanical energy. The ratio of the loss and storage moduli $tan\delta = E''/E'$ represents the ratio of the dissipated and stored mechanical energy in each loading cycle.

The temperature range of the DMA tests is from $-80^{\circ}C$ to $50^{\circ}C$, which covers the glass transition temperature ($T_g$), and most of the transition zone between the glassy state and the rubbery state. The sweeping frequencies are 20Hz, 10Hz, 5Hz, 2Hz and 1Hz. The nominal sample size for the DMA bending test is $3mm \times 10mm \times 30mm$, as shown in Fig. 1. The peak of the loss modulus is approximately at $T_g$, which is around -60 $^{\circ}C$, which is consistent with the results of the modulated differential scanning calorimetry (MDSC) [Holzworth et al., 2013].

During the test, the sample is cantilevered at both ends with a free length of 17.5 mm in between the clamps. One end of the sample is fixed, and the other end is attached to the movable clamp, which moves nomal to the axis of the beam sinusoidally with the amplitude of 15 $\mu$m. The data is collected for every $3^{\circ}C$. Followed by the stepwise increase, the thermal soaking time is 3 minutes for each temperature point, and liquid nitrogen is used to cool the system down to sub-ambient temperatures. One complete test with this protocol takes about 4.5 hours on TA 2980.

Multiple samples are tested for each material type. For pure polyurea and PUPMB composites (various volume fractions), we take average of three tests of three samples. Three samples from three different batches for pure polyurea; one sample from one batch and two samples from another batch for PUPMB. For PUMG composites (various volume fractions), one test for each volume fraction is shown in the paper, since we have independent extensive data on the effect of the surface treatment. 8 samples of each volume fraction have been tested, and the result shows the eight tests were the same within experimental error of DMA testing.

The storage and loss moduli DMA data of pure polyurea are shown in Fig. 2. Only the data above $T_g + 10^{\circ}C$ is presented here because relaxation mechanism varies near or below $T_g$. The storage and loss moduli of various volume fractions of PUPMB and PUMG at 1Hz are shown in Fig. 3. Pure polyurea and PUPMB_20% are shown as the average storage and loss moduli with the error bars representing the standard deviation. A complete set of PUMG DMA data will be shown in another paper, which is under preparation.

## 4 Frequency-domain master curves and the time-temperature superposition (TTS)

For most polymers, in the transition zone, increasing temperature has a similar effect on their mechanical properties as decreasing strain rate, and decreasing temperature has a similar effect as increasing strain rate. Thus, instead of testing the material in a wide frequency range, a substitute test can be conducted at a much narrower frequency range but at various temperatures. The materials' properties tested at various temperatures can be shifted to approximate the wide-frequency

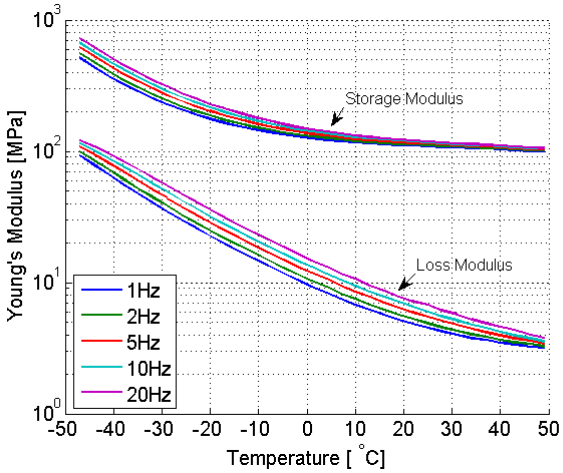


**Fig. 2** DMA data of storage and loss Young's moduli of pure polyurea

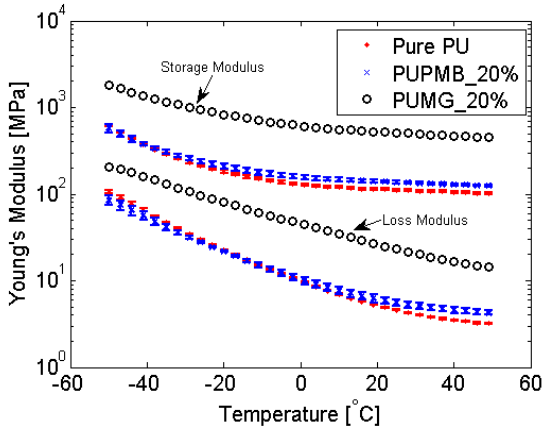


**Fig. 3** DMA 1Hz data for pure PU, PUPMB_20% and PUMG_20%. The error bars are shown for pure PU and PUPMB_20%.

response at a desired reference temperature. This empirical method is called time-temperature superposition (TTS) [Ferry, 1980].

Traditionally TTS involves both vertical and horizontal shifts for each modulus [Dealy and Plazek, 2009]:

$$E(\omega_r, T_0) = b(T, T_0)E(\omega, T) \tag{1}$$

$$\omega_r = a(T, T_0)\omega \tag{2}$$

where $T_0$ is the reference temperature, $T$ is the test temperature, $\omega$ is the test angular frequency, $\omega_r$ is the reduced angular frequency, $a(T, T_0)$ is the horizontal shift factor and $b(T, T_0)$ is the vertical shift factor.

In this work the Young's modulus of polyurea is directly shifted. It has been discussed in the literature [Guo et al., 2012, Grassia and D'Amore, 2008], that the bulk and shear response of polymers share the same temperature-frequency response at least at short time scales (around 5 decades below shear relaxation minimum). Some authors suggest that the bulk and shear transition ranges even span for the same number of decades [Park et al., 2005, Deng and Knauss, 1997, Arzoumanidis and Liechti, 2003]. For higher temperatures, the Young's modulus is dominated by the shear modulus ($E^* \simeq 3G^*$).

For the vertical shift, according to [Ferry, 1980] :

$$b(T, T_0) = \frac{T_0\rho_0}{T\rho} \tag{3}$$

Since the thermal expansion coefficient of polymers is of the order of $10^{-4}m/mK$, in the temperature range of interest, the effect of density change is negligible comparing to the effect of the temperature change. Thus in the following calculation we assume $\rho_0/\rho = 1$.

The horizontal shift factor $a(T, T_0)$ can be well fitted by the WLF equation in the material's transition zone:

$$log(a(T, T_0)) = \frac{-C_1(T - T_0)}{C_2 + (T - T_0)} \tag{4}$$

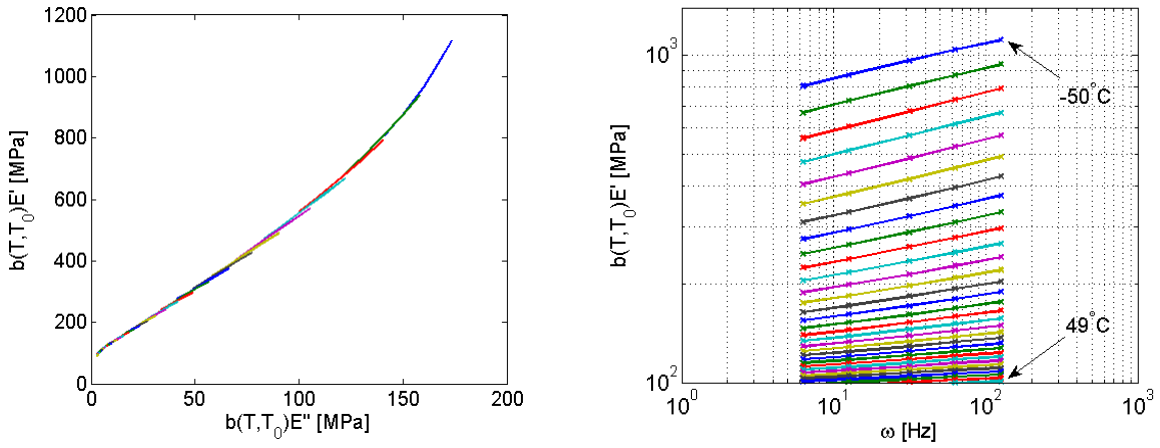


**Fig. 4** (a) Cole-Cole plot for pure polyurea. Temperature range is from $-50°C$ to $49°C$. Each color represents one temperature point and the temperature increment is $3°C$ between two neighboring lines. (b) DMA storage modulus of pure polyurea vs. angular frequency for temperatures from $-50°C$ to $49°C$, each color line represents $E'$ tested at one temperature point and at five frequencies. The difference between temperature points is $3°C$. The loss modulus plot has similar form.

Note that all the temperatures here are in absolute scale.

The storage and loss moduli are shifted independently. The two sets of shift factors, $log(a)$, are very close in numbers, which indicates the TTS may be performed in a reasonable way. The average shift factor is taken for developing the final master curves for both storage and loss moduli. The same shift factor may be used in time domain as well.

Only the DMA data above -50$°C$ are used for developing the viscoelastic models, since the classical TTS is usually applied for $T_g < T < T_g + 100°C$ [Williams et al., 1955]. $-50°C$ is sufficiently low for polyurea DMA data to approximate mechanical properties at frequencies as high as $10^{10}$ Hz.

A good indication that TTS is applicable for this type of material is the Cole-Cole plot, which plots the loss moduli $E''(\omega)$ against $E'(\omega)$, if all the data approximately lie on one line then the horizontal shift of TTS is applicable [Han and Kim, 1993]. Fig. 4 (a) shows the Cole-Cole plot of pure polyurea after storage and loss moduli have been vertically shifted by $b(T,T_0)$. As can be seen in the plot, almost all the data points lie on one line, only a small curvature is observed for low temperatures close to $T_g$.

The vertically shifted storage (as is shown in Fig. 4 (b)) and loss moduli are then horizontally shifted along the frequency axis to construct master curves. At each temperature $T_i$, data of the five test frequencies are linearly fitted as $y_i = c_i x + d_i$. The increment of the shift factor between two temperature points is defined as:

$$\Delta log[a(T_i, T_{i+1}, T_0)] = log[a(T_{i+1}, T_0)] - log[a(T_i, T_0)]$$

$(T_{i+1} = T_i - 3°C)$, and it is calculated as:

$$\Delta log[a(T_i, T_{i+1}, T_0)] = \frac{1}{2c_i.c_{i+1}} \cdot |(c_{i+1} - c_i)(c_{i+1}\omega_1 + \omega_m c_i) + (d_{i+1} - d_i)(c_{i+1} + c_i)|$$

which minimizes the horizontal overlapping area between isotherms of neighboring temperatures in Fig. 4 (b). Absolute value is taken for the robustness of the code. $[\omega_1, \omega_2, ...\omega_m]$ is the angular frequency table of the DMA test, which equals $2\pi \cdot [1,2,5,10,20]$ Hz in this study, and $[T_1, T_2, ...T_n]$ are the temperature points. $T_1$ is the highest temperature and $T_n$ is the lowest temperature.

The horizontal shift factor therefore is summed up with all the increments:

$$log[a(T, T_0)] = \sum_{i=1}^{n_T} \Delta log[a(T_i, T_{i+1}, T_0)] - \sum_{i=1}^{n_{T_0}} \Delta log[a(T_i, T_{i+1}, T_0)] \quad (5)$$

The first term of Eq. 5 is the summation from the highest temperature, and the second term adjusts the $log(a)$ to be zero for the reference temperature. $n_T$ is the index of the temperature array for the temperature $T$, and $n_{T_0}$ is the index for the reference temperature $T_0$.

The resultant horizontal shift factor and the master curves of pure polyurea are shown in Fig. 5 (a) and (b). In Fig. 5 (a), the logarithmic scale shift factor is fitted with the WLF model, at a reference temperature $T_0 = 0°C$, $C_1 = 32.95$ and $C_2 = 253.53K$. As can be seen in Fig. 5 (b), both storage and loss moduli form smoothly aligned master curves.

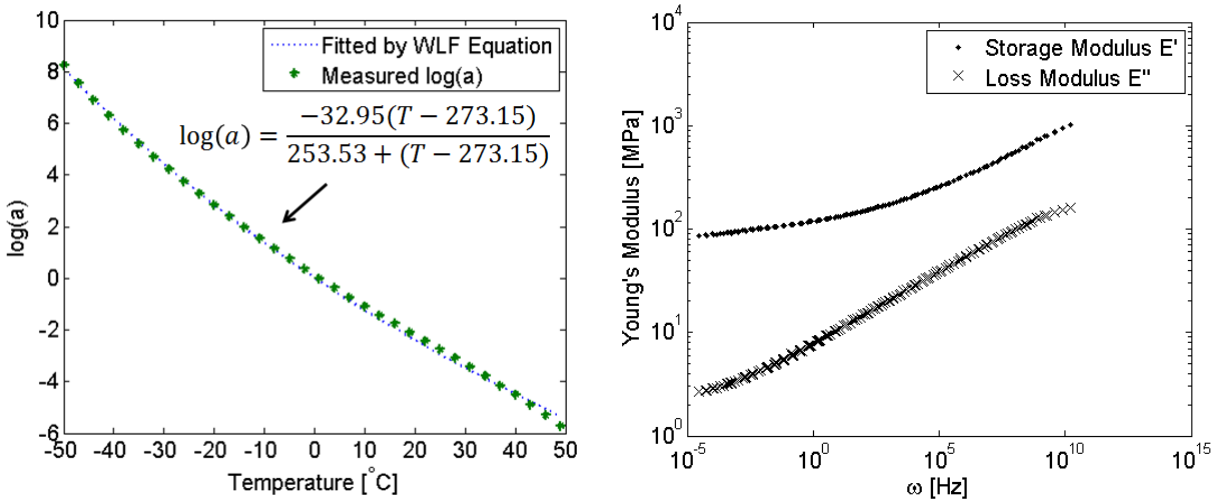


(a) (b)

**Fig. 5** (a) Horizontal shift factor for pure polyurea at reference temperature $T_0 = 0°C$, where $C_1 = 32.95$, and $C_2 = 253.53K$ for a very good WLF fit. (b) Master curves of pure polyurea at reference temperature $T_0 = 0°C$

## 5 Assessment of the quality of the master curves

### 5.1 Kramers-Kronig relations

The response of a physical system cannot precede the associated excitation in time due to causality. In linear systems, the response function relating the response to excitation may be transformed to the frequency domain. By Titchmarsh'theorem, this frequency domain function is analytical in the lower-half plane due to the causality considerations, when it is defined in the standard manner $F(\omega) = \frac{1}{2\pi}\int_{-\infty}^{\infty} f(t)e^{-i\omega t}dt$. The Kramers-Kronig relations are very useful consequences of this analyticity, relating the real and imaginary parts of the response function [Lucarini et al., 2004]. For viscoelastic material systems, the storage and loss moduli are interrelated by Kramers-Kronig relation as well, as shown in Eq. 6 - 7 [O'Donnell et al., 1981, Parot and Duperray, 2007, Booij and Thoone, 1982]:

$$E'(\omega) = E_{\omega\to\infty} + \frac{2}{\pi}\int_0^{\infty} \frac{uE''(u)}{\omega^2 - u^2}du \tag{6}$$

$$E''(\omega) = -\frac{2\omega}{\pi}\int_0^{\infty} \frac{E'(u)}{\omega^2 - u^2}du \tag{7}$$

In Ref. [O'Donnell et al., 1981], the relations were first derived for the bulk compliance, whereas they also apply for the elasticity moduli by changing the sign of each right-hand side. The integrals are understood as the Cauchy principal value and we also assume all are well-defined and limit all further analysis to viscoelastic solids with finite instantaneous response.

If the master curves represent the response function of a physical causal material system, the storage and loss moduli should follow the relations of Eq. 6-7. In order to calculate these integrals, the storage and loss moduli master curves must be extended to the frequency range of [0, ∞). Using the method in Ref. [Rouleau et al., 2013], the storage modulus is extended as an even function and the loss modulus is extended as a continuous odd function to ensure the time-domain relaxation modulus $E(t)$ is real. The master curves are represented by a set of piecewise linear functions, then the integrations can be carried out analytically for each linear segment.

$[\omega_1, \omega_2, ...\omega_n]$ and $[E_1^*, E_2^*, ...E_n^*]$ are the x and y data points of the smoothed experimental master curves. $[\Omega_0, \Omega_1, ...\Omega_{n+2}]$ and $[\bar{E}_0^*, \bar{E}_1^*, ...\bar{E}_{n+2}^*]$ are the new x and y data points of the extended master curves in [0, ∞), where $\bar{E}_i^* = \overline{E}_i' + i\overline{E}_i''$.

The data extension is as follows, and a schematic sketch is shown in the Fig. 6:

$$\Omega_0 = 0,\ \Omega_1 = \frac{\omega_1}{2}, ..., \ , \Omega_n = \frac{\omega_{n-1}+\omega_n}{2}, \Omega_{n+1} = \omega_n + \frac{\omega_n - \omega_{n-1}}{2},\ \Omega_{n+2} = +\infty$$

$$\overline{E}_0' = E_1',\ \overline{E}_1' = E_1',\ ...,\ \overline{E}_n' = \frac{E_{n-1}' + E_{n+1}'}{2}, \overline{E}_{n+1}' = E_n',\ \overline{E}_{n+2}' = E_n'$$

$$\overline{E}_0'' = 0,\ \overline{E}_1'' = \frac{E_1''}{2},\ ...,\ \overline{E}_n'' = \frac{E_{n-1}'' + E_{n+1}''}{2}, \overline{E}_{n+1}'' = 0,\ \overline{E}_{n+2}'' = 0$$

Each linear segment of storage modulus is approximated as:

$$E'(u) = a_i u + b_i, \Omega_i \leqq u < \Omega_{i+1},\ i = 0, 1, ...n+1.$$

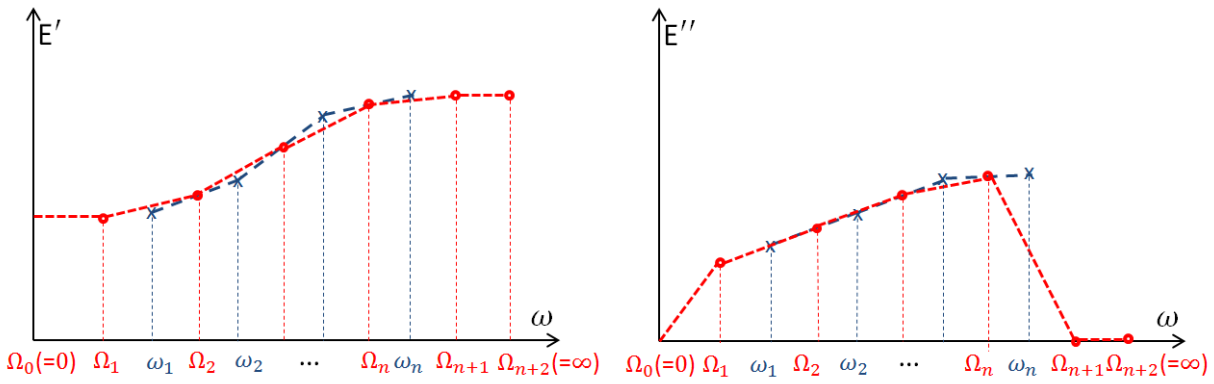


(a) (b)

**Fig. 6** Piecewise linear data extension to the $[0,\infty)$. (a) storage modulus master curve is extended as a even function. (b) loss modulus master curve is extended as an odd function

$$E''(u) = c_i u + d_i, \Omega_i \leqq u < \Omega_{i+1},\ i = 0,1,...n+1.$$

The adjustment on the data extension comparing to Ref. [Rouleau et al., 2013] is setting the loss modulus to zero instead of a constant for $\overline{E}''_{n+1}$ and $\overline{E}''_{n+2}$, since the intercept of the $n+1$ segment $d_{n+1}$ must equal zero for the integral (Eq. 6) to converge, thus its slope $c_{n+1}$ must equal zero for the loss modulus to be finite at infinite frequency. Note that for the last point of extension in storage modulus, up to 3% adjustment may be applied which is within the experimental error of DMA.

With this modification, the numerical integrations of Eq. 6 and 7 are (the same as in Ref.[Rouleau et al., 2013]):

$$E'(\omega) - E_{\omega\to\infty} = -\frac{2c_0}{\pi}\Omega_1 - \frac{\omega c_0}{\pi} ln\left|\frac{\Omega_1-\omega}{\Omega_1+\omega}\right| - \sum_{i=1}^{n}\left[\frac{2c_i}{\pi}(\Omega_{i+1}-\Omega_i) + \frac{\omega c_i}{\pi} ln\left|\frac{(\Omega_{i+1}-\omega)(\Omega_i+\omega)}{(\Omega_{i+1}+\omega)(\Omega_i-\omega)}\right| + \frac{d_i}{2} ln\left|\frac{\Omega_{i+1}^2-\omega^2}{\Omega_i^2-\omega^2}\right|\right]$$

$$E''(\omega) = \frac{b_0}{\pi} ln\left|\frac{\Omega_1-\omega}{\Omega_1+\omega}\right| + \sum_{i=1}^{n}\left[\frac{\omega a_i}{\pi} ln\left|\frac{\Omega_{i+1}^2-\omega^2}{\Omega_i^2-\omega^2}\right| + \frac{b_i}{\pi} ln\left|\frac{(\Omega_{i+1}-\omega)(\Omega_i+\omega)}{(\Omega_{i+1}+\omega)(\Omega_i-\omega)}\right|\right] + \frac{b_{n+1}}{\pi} ln\left|\frac{\Omega_{n+1}+\omega}{\Omega_{n+1}-\omega}\right|$$

By comparing the storage modulus master curve with the one calculated from loss modulus via this technique, and similarly by comparing the loss modulus master curve with the one calculated from storage modulus, the quality of the master curves developed by TTS can be assessed. For pure polyurea, Fig. 7 shows the master curves agree well with Kramers-Kronig relations except for a few points at the two ends of very low and very high frequencies. The difference at the low and high frequencies is due to the lack of information outside the frequency range of the experimental data. Similar results have been observed in other publications [Parot and Duperray, 2007]. More will be discussed in the discussion section.

## 5.2 Verification by ultrasonic wave test

Ultrasonic longitudinal and shear wave tests are conducted at 1MHz to compare with the master curves. Same method was used to measure the longitudinal and shear moduli in Ref. [Qiao et al., 2011], while new test data with less noise are reported here. Two samples of different thicknesses ($d_1$ and $d_2$) are tested and the wave speed and attenuation are measured. The real and imaginary part of both longitudinal and shear moduli are calculated as:

$$M' = \frac{\rho c^2(1-r^2)}{(1+r^2)^2} \tag{8}$$

$$M'' = \frac{2\rho c^2 r}{(1+r^2)^2} \tag{9}$$

where $r = \alpha c/\omega$, $\alpha$ is the attenuation, and $c$ is the wave speed.

$$\alpha = \frac{1}{d} ln(A_1/A_2) \tag{10}$$

.

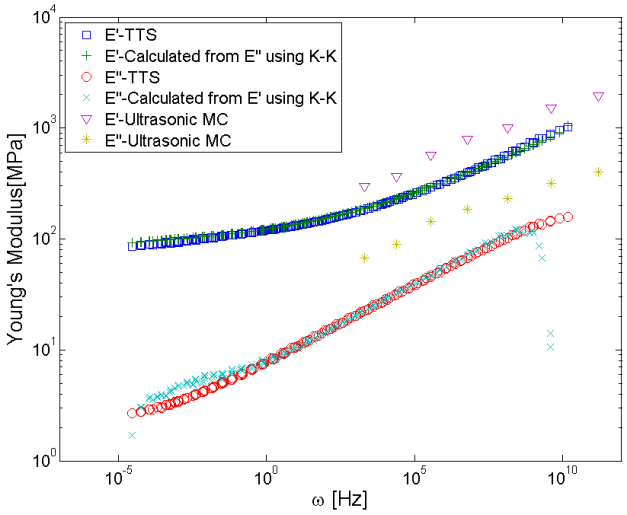


**Fig. 7** Master curve quality check by Kramers-Kronig relations and ultrasonic wave test for pure polyurea at 0 °*C*.

$A_1$ is the amplitude of the received signal measured through the thin sample with the thickness $d_1$, and $A_2$ is the amplitude measured through the thick sample with the thickness $d_2$, and $d = d_2 - d_1$. $M'$ and $M''$represent either longitudinal or shear moduli depending on whether longitudinal or shear waves are considered. The complex Young's modulus is calculated from the shear modulus $G^*$ and longitudinal modulus $L^*$ as:

$$E^* = \frac{G^*(3L^* - 4G^*)}{L^* - G^*} \tag{11}$$

The storage and loss Young's moduli obtained by ultrasonic wave test are then shifted vertically and also by using the horizontal shift factor $log(a)$ measured form the TTS of DMA data. This ultrasonic master curve is compared with the DMA master curves in Fig. 7. Due to the fact that the ultrasonic wave testing at various temperatures is extremely time-consuming, only one set of samples (for longitudinal and shear wave testing) is tested for each material type. As can be seen in Fig. 7 and two additional examples for polyurea composites in Fig. 11, the ultrasonic storage modulus matches well with the DMA master curves in general, while the ultrasonic loss modulus is higher than the DMA master curves, which is hypothesized to be due to the local resonance in the material [Qiao et al., 2011].

## 6 Relaxation spectra and Prony series

### 6.1 Relaxation spectra

Relaxation spectra represent how all the relaxation mechanisms with different relaxation times contribute to the overall stiffness of the material.

The relation of relaxation spectrum $H$ and relaxation modulus $E(t)$ is [Ferry, 1980]:

$$E(t) = E_e + \int_0^\infty H(\tau) e^{-t/\tau} dln\tau \tag{12}$$

here $E_e$ represents the equilibrium modulus when $t \to \infty$. The storage and loss moduli in frequency domain can also be calculated from the relaxation spectrum as:

$$E' = E_e + \int_0^\infty [H(\tau)\omega^2\tau^2/(1+\omega^2\tau^2)] dln\tau \tag{13}$$

$$E'' = \int_0^\infty [H(\tau)\omega\tau/(1+\omega^2\tau^2)] dln\tau \tag{14}$$

The relaxation spectrum may be approximated from the storage and loss moduli though various methods, including continuous relaxation spectrum calculation [Ferry and Williams, 1952, Ferry, 1980, Schwarzl and Staverman, 1952] or numerical calculation for discrete relaxation spectrum [Baumgaertel and Winter, 1989, Winter, 1997, Stadler and Bailly, 2009]. The former method includes emperical assumptions and the latter involves relative complex programming to tackle the ill-posed problem of direct fitting from the frequency domain. For simplicity, as one part of our entire computational code, we incorporated the method by [Ferry and Williams, 1952], and it provides good accuracy for various polyurea and polyurea-based composites. For other more complex material systems, if needed, there are other methods available.

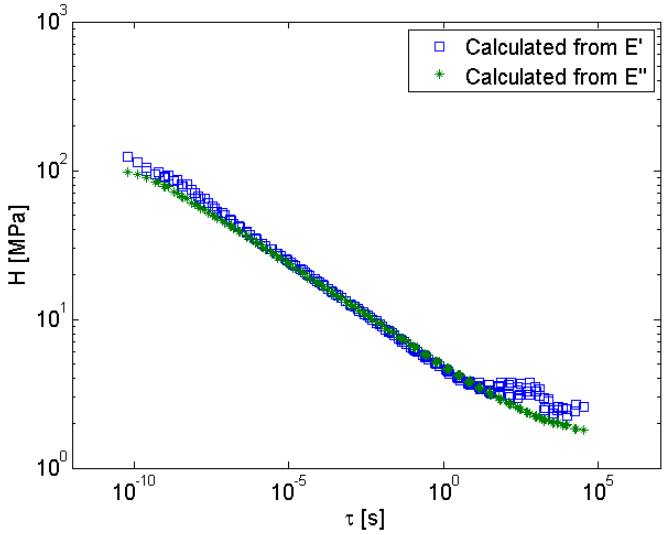


**Fig. 8** Relaxation spectra of pure polyurea at $0°C$

A first estimation of the relaxation spectrum is performed using the storage and loss moduli master curves. The method is summarized in Eq. 15-19 [Ferry and Williams, 1952]:

$$H_A(\tau) \simeq E' \left( \frac{\mathrm{d}logE'}{\mathrm{d}log\omega} \right) \Bigg|_{1/\omega=\tau} \tag{15}$$

$$H_B(\tau) \simeq E'' \left(1 - \frac{\mathrm{d}logE''}{\mathrm{d}log\omega}\right) \Bigg|_{1/\omega=\tau} \tag{16}$$

Then the result of the first estimation is used to calculate the adjustment factors $m_A$, $m_B$, $A$ and $B$.

$$m_A = \frac{\mathrm{d}logH_A}{\mathrm{d}log\tau}, \; m_B = \frac{\mathrm{d}logH_B}{\mathrm{d}log\tau} \tag{17}$$

$$A = \frac{1+|m_A-1|}{2\Gamma\left(2-\frac{m_A}{2}\right)\Gamma\left(1+\frac{m_A}{2}\right)}, -2 \le m \le 2$$

$$B = \frac{1+|m_B|}{2\Gamma\left(\frac{3}{2}-\left|\frac{m_B}{2}\right|\right)\Gamma\left(\frac{3}{2}+\left|\frac{m_B}{2}\right|\right)}, -1 \le m \le 3$$

where $\Gamma$ represents the Gamma Function $\Gamma(t) = \int_0^\infty x^{t-1}e^{-x}dx$. With these adjustment factors, the second approximation of $H$ is calculated as:

$$H_A(\tau) = AE' \left(1 - \left| \frac{\mathrm{d}logE'}{\mathrm{d}log\omega} - 1 \right| \right) \Bigg|_{1/\omega=\tau} \tag{18}$$

$$H_B(\tau) = BE'' \left(1 - \left| \frac{\mathrm{d}logE''}{\mathrm{d}log\omega} \right| \right) \Bigg|_{1/\omega=\tau} \tag{19}$$

If the storage and loss moduli master curves have good inherent consistency, Eq. 18 and 19 should give the same or similar relaxation spectra. Representative relaxation spectra for pure polyurea at $0°C$ are shown in Fig. 8. The blue square curve is the relaxation spectrum calculated from storage modulus $E'$, and the green star curve is the relaxation spectrum calculated from loss modulus $E''$. Besides Kramers-Kronig relations and the ultrasonic test verification, the similarity of the two relaxation spectra is another piece of evidence that the master curves of storage and loss moduli developed from TTS have good inherent consistency.

In the relaxation spectrum calculations, all the derivatives are calculated by taking the slope of the linear fitting of the neighboring 11 data points (5 points on the left and 5 points on the right).

## 6.2 Prony series

### *6.2.1 High-resolution Prony series*

The discrete form of Eq. 12 is the Prony series

$$E(t) = E_e + \sum_{i=1}^{n} E_i e^{-t/\tau_i} \tag{20}$$

where $E_i$ and $\tau_i$ are the stiffness and relaxation time of the $i^{th}$ Maxwell dash pot-spring element [Ferry, 1980]. In the frequency domain it can be easily written as:

$$E'(\omega) = E_e + \sum_{i=1}^{n} E_i \frac{\omega^2 \tau_i^2}{1+\omega^2 \tau_i^2} \tag{21}$$

$$E''(\omega) = \sum_{i=1}^{n} E_i \frac{\omega \tau_i}{1+\omega^2 \tau_i^2} \tag{22}$$

If sufficient number of terms are used, Eq. 21-22 should be able to represent the master curve with good accuracy. By using the same set of high-resolution $E_i$ and $\tau_i$, the relaxation modulus Eq. 20 can be obtained. For the best accuracy of the relaxation modulus, the maximum number of terms is used, such that the number of Prony terms is equal to the number of data points in the frequency-domain master curve.

Starting with the relaxation spectrum data, the magnitude of each Prony term is approximated as:

$$E_i = H(\tau_i)(ln\tau_{i+1} - ln\tau_i)|_{\omega_i = 1/\tau_i} \tag{23}$$

where $\tau_i$ and $H(\tau_i)$ are the x and y axes of the $i^{th}$ data point of the relaxation spectrum shown in Fig. 8, and assuming $\tau_{i+2}$ exists and $ln\tau_{i+2} - ln\tau_{i+1} = ln\tau_{i+1} - ln\tau_i$.

The equilibrium storage modulus $E_e$ is calculated as:

$$E_e = \frac{1}{n} \sum_{i=1}^{n} \left[ E'(\omega_i) - \sum_{j=1}^{n} E_j \frac{\omega_i^2 \tau_j^2}{1+\omega_i^2 \tau_j^2} \right] \tag{24}$$

The master curves plotted by the high-resolution Prony series (Eq. 21-22, with maximum n) lie on top of the master curves developed from TTS. Note that although $E'$ values are used directly, the major portion of data is extracted from the relaxation spectrum H which was just shown to be the same function regardless of whether one starts from $E'$ or $E''$ master curves.

This section further insures that the relaxation modulus can accurately represent information of the frequency domain master curves at all frequencies except for the two ends near 0 and infinite frequencies, where experimental information is deficient.

Time-domain Young's modulus of polyurea can also be well represented in this power-law form [Amirkhizi et al., 2006]:

$$E(t,T) = \frac{T}{T_0} \left( E_{t\to\infty} + \Delta E \left( \frac{t}{a(T)} \right)^{-\theta} \right) \tag{25}$$

The unit of time $t$ is in seconds. At the reference temperature, Eq. 25 becomes the time-domain master curve:

$$E(t, T = T_0) = E_{t\to\infty} + \Delta E t^{-\theta} \tag{26}$$

For pure polyurea at reference temperature $0^{\circ}C$, the three parameters are fitted as:

$$E_{t\to\infty} = 78.46MPa$$

$$\Delta E = 32.45MPa$$

$$\theta = 0.1396$$

As can be seen in Fig. 9, this power-law expression (Eq. 26) can represent the time-domain master curve very well. The only shortcoming of this representation is that for explicit finite element calculations there is no straightforward algorithm for incremental time integration.

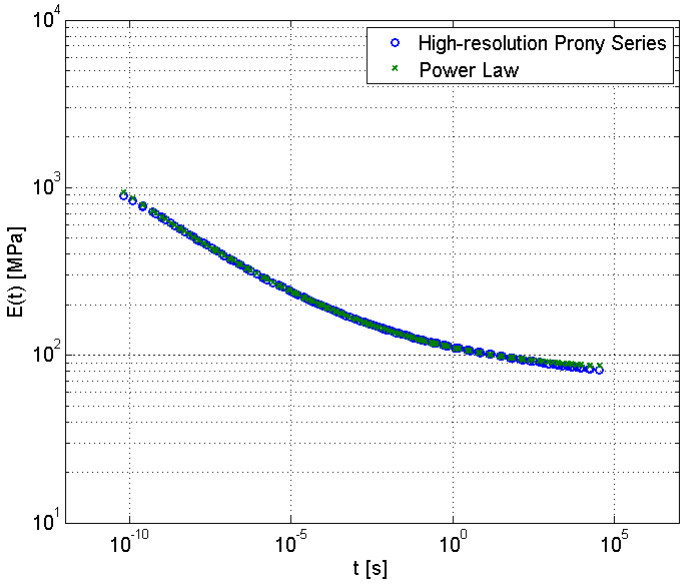


**Fig. 9** Power law compared with high-resolution Prony series for pure polyurea.

| $E_i$ | [MPa] | $\tau_i$ | [s] |
|---|---|---|---|
| $E_e$ | 126.48 | $\tau_e$ | $\infty$ |
| $E_1$ | 194.63 | $\tau_1$ | 5.05E-09 |
| $E_2$ | 123.71 | $\tau_2$ | 7.00E-08 |
| $E_3$ | 82.60 | $\tau_3$ | 8.40E-07 |
| $E_4$ | 51.90 | $\tau_4$ | 8.21E-06 |
| $E_5$ | 37.84 | $\tau_5$ | 6.82E-05 |
| $E_6$ | 28.04 | $\tau_6$ | 5.10E-04 |
| $E_7$ | 16.86 | $\tau_7$ | 3.46E-03 |
| $E_8$ | 21.72 | $\tau_8$ | 2.14E-02 |

**Table 1** 8-term Prony series to approximate the pure polyurea properties within the range of $10^2 - 10^8$Hz at $0^\circ C$.

### *6.2.2 Customized reduced-term Prony series*

However, more than 100 Prony terms make this high-resolution Prony series hard to use on the actual computational platforms. Thus a further step is taken to reduce the number of Prony terms while maintaining the usefulness of the Prony series. We call this step a customizing procedure, in other words, we create a customized Prony series suitable for a limited frequency range of interest for the specific computational problem to obtain both good accuracy and low compuational cost.

Usually Prony series of 4-8 terms can be conveniently applied in computational platforms. This reduced term Prony series can be calculated by applying the least square fitting using the time domain relaxation modulus.

Assuming the frequency range of interest for the computational problem is $\omega_{min} < \omega < \omega_{max}$, the corresponding time range is $t_{min} = \frac{1}{\omega_{max}} < t < \frac{1}{\omega_{min}} = t_{max}$. The data points of time within this range are $[t_1, t_2, ..., t_m]$, and the relaxation times $[\tau_1, \tau_2, ..., \tau_p]$ can be assigned as equally spaced in the logarithmic scale within this time range. Given the relatively flat spectrum for these polymers, the equidistant choice of discrete times is a reasonable choice. Then the optimized amplitude of each Prony term can be calculated as:

$$\begin{bmatrix} E_e \\ E_1 \\ \vdots \\ E_p \end{bmatrix} = (A^T A)^{-1} A^T \begin{bmatrix} E(t_1) \\ E(t_2) \\ \vdots \\ E(t_m) \end{bmatrix}, \; where\, A = \begin{bmatrix} 1 & e^{-t_1/\tau_1} & \cdots & e^{-t_1/\tau_p} \\ 1 & e^{-t_2/\tau_1} & \cdots & e^{-t_2/\tau_p} \\ \vdots & \vdots & \vdots & \vdots \\ 1 & e^{-t_m/\tau_1} & \cdots & e^{-t_m/\tau_p} \end{bmatrix}_{m \times p}$$

An example of 8-term Prony series is shown in Fig. 10 (a) and (b) for the frequency range from $10^2$ to $10^8$ Hz. The parameters of this 8-term Prony series are listed in Table 1.

## 7 Example results for polyurea based composites

The same method of TTS has been applied for many polyurea-based composite systems. Two examples are polyruea with milled glass (PUMG), and polyurea with phenolic microbubbles (PUPMB). The master curves of TTS are compared with

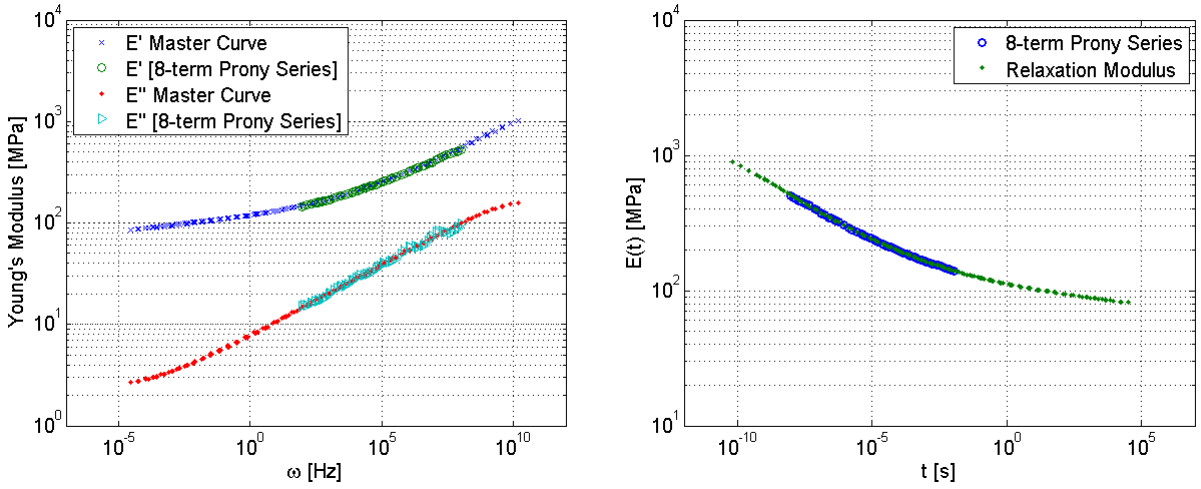


(a) (b)

**Fig. 10** (a) Master curves and Prony series approximation at $10^2 - 10^8$Hz for pure polyurea at $0°C$ (b) Relaxation modulus and Prony series approximation at $10^2 - 10^8$Hz for pure polyurea at $0°C$

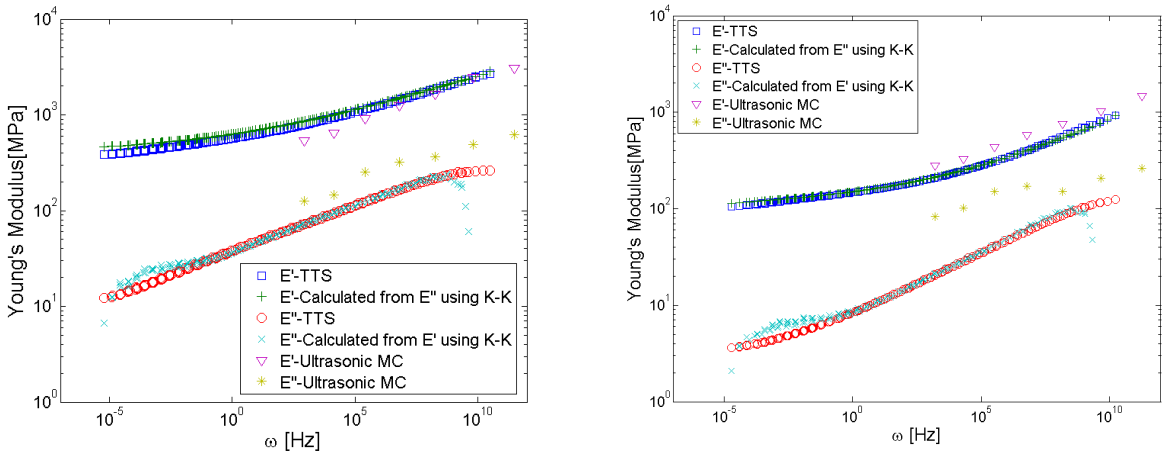


(a) (b)

**Fig. 11** (a) Master curve quality check by Kramers-Kronig relations and ultrasonic wave test for polyurea with 20% volume fraction of milled glass at 0 $°C$. (b) Master curve quality check by Kramers-Kronig relations and ultrasonic wave test for polyurea with 20% volume fraction of phenolic microbubbles at 0 $°C$.

| Material Name | $E_{t\to\infty}$ [MPa] | $\Delta E$ [MPa] | $\theta$ |
|---|---|---|---|
| Pure PU | 78.46 | 32.45 | 0.1396 |
| PUMG_10% | 156.11 | 95.25 | 0.1167 |
| PUMG_15% | 197.86 | 135.46 | 0.1088 |
| PUMG_20% | 283.14 | 239.04 | 0.0949 |
| PUPMB_10% | 89.74 | 34.77 | 0.1327 |
| PUPMB_20% | 95.63 | 39.42 | 0.1247 |
| PUPMB_30% | 102.93 | 43.02 | 0.1184 |
| PUPMB_40% | 106.63 | 54.89 | 0.1059 |

**Table 2** Power law parameters for pure polyurea, PUMG and PUPMB for reference temperature at $0°C$.

both ultrasonic data and are checked by the Kramers-Kronig relations, as shown in Fig 11. Similar to what is observed for pure polyurea in Fig. 7, higher loss modulus of ultrasonic measurement and Kramers-Kronig relation edge effect are observed. The relaxation moduli of pure polyurea, PUMG and PUPMB are shown in Fig. 12.

The power law (Eq. 26 ) parameters for pure polyurea, PUMG and PUPMB are summarized in Table 2. These power law parameters can be used to plot the relaxation moduli (shown in Fig. 12) for calculating the optimized parameters of the Prony series.

The WLF parameters $C_1$ and $C_2$ for pure polyuera, PUMG, and PUPMB are summarized in Table 3.

8-term Prony series for PUMG (volume fraction 10%,15%, 20%) and PUPMB (volume fraction 10%, 20%, 30%, 40%) are also calculated for the frequency range of $10^2 - 10^8$Hz at $0°C$, and the numbers can be found in the supplementary material of this paper.

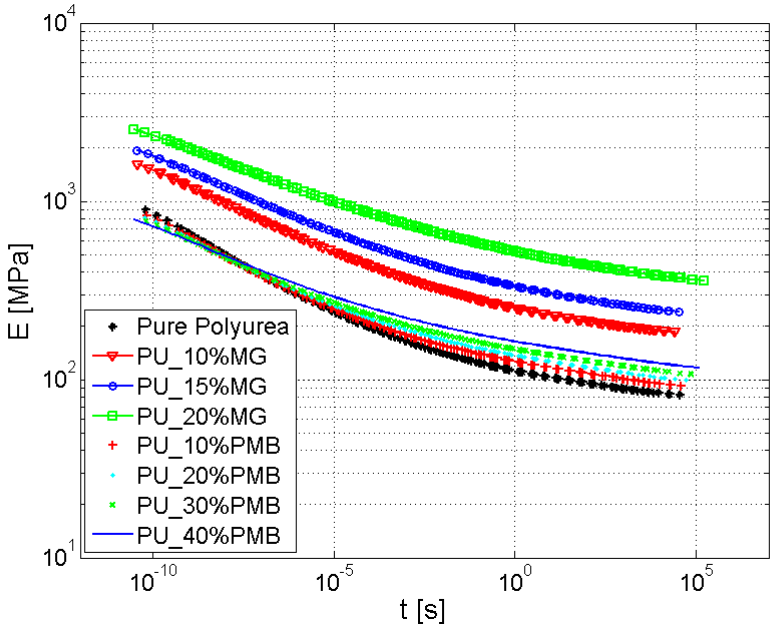


**Fig. 12** Relaxation modulus $E(t)$ of PUMG and PUPMB composites at varying volume fractions. All curves at reference termperature $T_0 = 0°C$.

| Material Name | $C_1$ | $C_2[K]$ |
|---|---|---|
| Pure PU | 32.95 | 253.53 |
| PUMG_10% | 29.39 | 227.15 |
| PUMG_15% | 31.09 | 237.015 |
| PUMG_20% | 44.98 | 317.83 |
| PUPMB_10% | 33.89 | 260.31 |
| PUPMB_20% | 36.15 | 272.42 |
| PUPMB_30% | 39.60 | 294.95 |
| PUPMB_40% | 41.42 | 295.88 |

**Table 3** WLF parameters $C_1$ and $C_2$ for pure polyurea, PUMG and PUPMB for reference temperature at $0°C$.

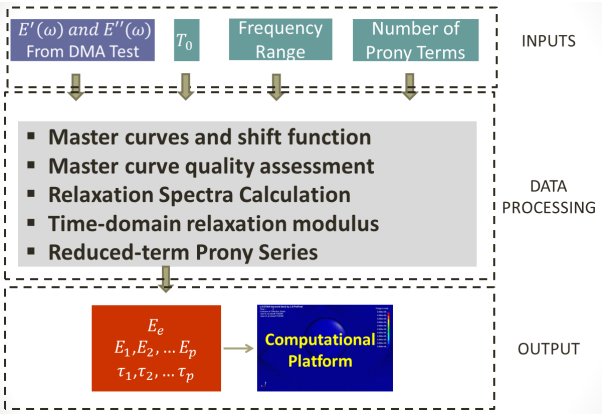


**Fig. 13** Method summary

## 8 Summary and discussion

This study developed a consistent method to obtain Prony series of polyurea and polyurea-based composites using the DMA test data.

A flowchart of the method is shown in Fig. 13. The four inputs of this method are the DMA test data, reference temperature $T_0$, frequency range of interest and the number of Prony terms. We have developed a computer code that automatically processes the data including the master curve development by time-temperature superposition, creates graphs for quality assessment of the master curves, and finally performs relaxation spectra calculation, time-domain relaxation modulus calculation, and the reduced-term Prony series calculation. This method gives an efficient constitutive model, which gives good accuracy while maintaining the low computational cost.

After the data processing platform is constructed, the most effort for getting a shear viscoelastic constitutive model remains in the sample fabrication and DMA test. The data processing takes negligible time on a regular PC, and it gives

the reduced-term Prony series that can be directly used in finite element explicit codes. Other necessary information can also be acquired through the data processing, including the shift factor $log(a)$, which represents the temperature effect on the material relaxation mechanism, and has to be incorporated to consider the temperature change in some adiabatic deformation [Amirkhizi et al., 2006].

Regarding the applicability of TTS to polyurea and polymer composites, different opinions exit [Roland et al., 2007]. Due to the phase separation in the polyurea and the heterogeneity in the microstructure of polymer composites, not all components in the material share the same set of relaxation mechanisms, and that is the main reason to question the applicability of TTS. However, this does not completely exclude TTS as a useful empirical estimation for copolymers like polyurea when substitute tests are not easily available.

The hard domains of polyurea are nanometer size [Castagna et al., 2012], and the $T_g$ of the hard domain is significantly higher than the soft domain [Rinaldi et al., 2011], we expect most of the relaxation happens in the soft domain for most of the frequencies, while for the extremely high frequency above $10^9$ Hz, some energy may go into the local resonance due to the existence of the hard domains. For most applications, $10^9$ Hz is high enough. The master curves may still be a good starting point for those extremely high strain rate problem to use as a computational guidance.

For polyruea composites, the reliable frequency range of the master curves needs to be estimated based on the size, mass and distribution of the inclusions. For the composites examples of PUMG and PUPMB, due to the micrometer size inclusions, the master curves are more reliable in the lower frequency range. For example, their master curves can be used for acoustic problems.

The verification by the Kramers-Kronig relations shows the master curves of storage and loss moduli are interrelated and are representing a causal physical system. The discrepancy at the two frequency ends of the loss modulus does not mean the master curves are not reliable at low and high frequencies. It is actually related with how the experimental data are extrapolated to $\omega \in [0,\infty)$. By changing the way of data extension, i.e., adjusting the value of the $E'(\omega = \infty)$, and moving the positions of $\Omega_1$ and $\Omega_{n+1}$ to be closer to the physical case, or possibly changing the piecewise linear extrapolation to higher order, the discrepancy of the calculated loss modulus may be reduced.

The method discussed in this paper can also be applied for other polymers. The temperature range of the DMA test needs to be determined for other polymers and the reference temperature needs to lie in the temperature range of the TTS. Experience shows the Young's moduli tested by single-cantilever bending and thin-film tension tests are almost the same for polyurea on TA2980, as long as appropriate tests are conducted within the machine's test range. If the available sample size is small, a thin-film tension test can replace the single-cantilever bending test.

## 9 Acknowledgments

This work has been supported by the Office of Naval Research (ONR) grant N00014-09-1-1126 to the University of California, San Diego, and also ONR grant N00014-13-1-0392 to the University of Massachusetts, Lowell.

## References

A. V. Amirkhizi, J. Isaacs, J. McGee, and S. Nemat-Nasser. An Experimentally-based Viscoelastic Constitutive Model for Polyurea, Including Pressure and Temperature Effects. *Philosophical Magazine*, 86(36):5847–5866, December 2006.

G. A. Arzoumanidis and K. M. Liechti. Linear viscoelastic property measurement and its significance for some nonlinear viscoelasticity models. *Mechanics of Time-Dependent Materials*, 7(3-4):209–250, 2003.

M. Baumgaertel and H. H. Winter. Determination of discrete relaxation and retardation time spectra from dynamic mechanical data. *Rheologica Acta*, 28(6):511–519, 1989.

H. C. Booij and G. Thoone. Generalization of Kramers-Kronig Transforms and Some Approximations of Relations Between Viscoelastic Quantities. *Rheologica Acta*, 21(1):15–24, 1982.

M. Broekaert. *Polyurea Spray Coatings - The Technology and Latest Development*. Huntsman Polyurethanes, B3078 Everberg, Belgium, 2002.

A. M. Castagna, A. Pangon, T. Choi, G. P. Dillon, and J. Runt. The Role of Soft Segment Molecular Weight on Microphase Separation and Dynamics of Bulk Polymerized Polyureas. *Macromolecules*, 45(20):8438–8444, October 2012.

J. Dealy and D. Plazek. Time-temperature Superposition - A Users Guide. *Rheology Bulletin*, 78(2):16–31, 2009.

T. H. Deng and W. G. Knauss. The temperature and frequency dependence of the bulk compliance of poly(vinyl acetate). an re-examination. *Mechanics of Time-Dependent Materials*, 1:33–49, 1997.

J. D. Ferry. *Viscoelastic Properties of Polymers*. 1980.

J. D. Ferry and M. L. Williams. Second Approximation Methods for Determining the Relaxation Time Spectrum of a Viscoelastic Material. *Relaxation Spectrum of Viscoelastic Materials*, pages 347–353, 1952.

L. Grassia and A. D'Amore. The relative placement of linear viscoelastic functions in amorphous glassy polymers. *Journal of Rheology*, 53:339–356, 2008.

M. Grujicic, B. Pandurangan, T. He, B. A. Cheeseman, C. F. Yen, and C. L. Randow. Computational Investigation of Impact Energy Absorption Capability of Polyurea Coatings via Deformation-induced Glass Transition. *Materials Science and Engineering: A*, 527(29-30):7741–7751, November 2010.

J. Guo, J. Grassia, and Simon S. L. Bulk and Shear Rheology of a Symmetric Three-Arm Star Polystyrene. *Polymer Physics*, 50(1):1233–1244, 2012.

C. D. Han and J. D. Kim. On the Use of Time-temperature Superposition in Multicomponent/ Multiphase Polymer Systems. *Polymer*, 34(12):2533–2539, 1993.

K. Holzworth, Z. Jia, A. V. Amirkhizi, J. Qiao, and S. Nemat-Nasser. Effect of Isocyanate Content on Thermal and Mechanical Properties of Polyurea. *Polymer*, 54(12):3079–3085, May 2013.

V. Lucarini, J.J. Saarinen, K. E. Peiponen, and E.M. Vartiainen. *Kramers-Kronig Relations in Optical Materials Research*. Springer, 2004.

M. O'Donnell, E. T. Jaynes, and J. G. Miller. Kramers-Kronig Relationship Between Ultrasonic Attenuation and Phase Velocity. *Journal of Acoustical Society of America*, 69(3):696–701, 1981.

S. J. Park, K. M. Liechti, and S. Roy. Simplified Bulk Experiments and Hygrothermal Nonlinear Viscoelasticity. *Mechanics of Time-Dependent Materials*, 8:303–344, 2005.

J. M. Parot and B. Duperray. Applications of Exact Causality Relationships to Materials Dynamic Analysis. *Mechanics of Materials*, 39(5):419–433, May 2007.

J. Qiao, A. V. Amirkhizi, K. Schaaf, S. Nemat-Nasser, and G. Wu. Dynamic Mechanical and Ultrasonic Properties of Polyurea. *Mechanics of Materials*, 43(10):589–607, 2011.

R. G. Rinaldi, M. C. Boyce, S. J. Weigand, D. J. Londono, and M. W. Guise. Microstructure Evolution During Tensile Loading Histories of a Polyurea. *Journal of Polymer Science Part B: Polymer Physics*, 49(23):1660–1671, December 2011.

C. M. Roland and R. Casalini. Effect of Hydrostatic Pressure on the Viscoelastic Response of Polyurea. *Polymer*, 48(19): 5747–5752, September 2007.

C. M. Roland, J. N. Twigg, Y. Vu, and P. H. Mott. High Strain Rate Mechanical Behavior of Polyurea. *Polymer*, 48(2): 574–578, January 2007.

L. Rouleau, J.-F. Deü, A. Legay, and F. L. Lay. Application of Kramers-Kronig Relations to Time-temperature Superposition for Viscoelastic Materials. *Mechanics of Materials*, 65:66–75, October 2013.

S. S. Sarva, S. Deschanel, M. C. Boyce, and W. Chen. Stress-strain Behavior of a Polyurea and a Polyurethane from Low to High Strain Rates. *Polymer*, 48(8):2208–2213, April 2007.

F. Schwarzl and A. J. Staverman. Higher approximations of relaxation spectra. *Physica*, 18(10):791–798, 1952.

F. J. Stadler and C. Bailly. A new method for the calculation of continuous relaxation spectra from dynamic-mechanical data. *Rheologica Acta*, 48(1):33–49, 2009.

M. L. Williams, R. F. Landel, and J. D. Ferry. The Temperature Dependence of Relaxation Mechanisms in Amorphous Polymers and Other Glass-forming Liquids. *Journal of the American Chemical Society*, 77:3701–3707, 1955.

H. H. Winter. Analysis of dynamic mechanical data: inversion into a relaxation time spectrum and consistency check. *Journal of Non-Newtonian Fluid Mechanics*, 68(2):225–239, 1997.